THE JOURNAL OF BIOLOGICAL CHEMISTRY VOL. 285, NO. 2, pp. 1177–1187, January 8, 2010

Conditional Disruption of *Pkd1* in Osteoblasts Results in Osteopenia Due to Direct Impairment of Bone Formation*

Received for publication, July 30, 2009, and in revised form, October 23, 2009 Published, JBC Papers in Press, November 3, 2009, DOI 10.1074/jbc.M109.050906

Zhousheng Xiao, Shiqin Zhang, Li Cao, Ni Qiu, Valentin David, and L. Darryl Quarles[1]

From the Kidney Institute, University of Kansas Medical Center, Kansas City, Kansas 66160

PKD1 (polycystin-1), the disease-causing gene for ADPKD, is widely expressed in various cell types, including osteoblasts, where its function is unknown. Although global inactivation of *Pkd1* in mice results in abnormal skeletal development, the presence of polycystic kidneys and perinatal lethality confound ascertaining the direct osteoblastic functions of PKD1 in adult bone. To determine the role of PKD1 in osteoblasts, we conditionally inactivated *Pkd1* in postnatal mature osteoblasts by crossing *Oc* (osteocalcin)-Cre mice with floxed *Pkd1* (*Pkd1*$^{flox/m1Bei}$) mice to generate conditional heterozygous (*Oc*-Cre;*Pkd1*$^{flox/+}$) and homozygous (*Oc*-Cre;*Pkd1*$^{flox/m1Bei}$) *Pkd1*-deficient mice. Cre-mediated recombination (*Pkd1*$^{\Delta flox}$) occurred exclusively in bone. Compared with control mice, the conditional deletion of *Pkd1* from osteoblasts resulted in a gene dose-dependent reduction in bone mineral density, trabecular bone volume, and cortical thickness. In addition, mineral apposition rates and osteoblast-related gene expression, including *Runx2*-II (Runt-related transcription factor 2), osteocalcin, osteopontin, and bone sialoprotein, were reduced proportionate to the reduction of *Pkd1* gene dose in bone of *Oc*-Cre;*Pkd1*$^{flox/+}$ and *Oc*-Cre;*Pkd1*$^{flox/m1Bei}$ mice. Primary osteoblasts derived from *Oc*-Cre;*Pkd1*$^{flox/m1Bei}$ displayed impaired differentiation and suppressed activity of the phosphatidylinositdol 3-kinase-Akt-GSK3β-β-catenin signaling pathways. The conditional deletion of *Pkd1* also resulted in increased adipogenesis in bone marrow and in osteoblast cultures. Thus, PKD1 directly functions in osteoblasts to regulate bone formation.

PC1 (polycystin-1) is a highly conserved, receptor-like multidomain membrane protein widely expressed in various cell types and tissues (1, 2). Mutations of human *PKD1* (polycystic kidney disease gene 1) cause autosomal dominant polycystic kidney disease (ADPKD)[2] (3, 4). The genetics of ADPKD is complex, because it is widely held that inactivation of the normal copy of the *PKD1* gene by a second somatic mutation in conjunction with the inherited mutation of the other allele is required for renal cyst formation, which occurs in only a subset of the dually affected tubules (5). Although primarily affecting the kidney, ADPKD is also a multisystem disorder (6, 7). Extrarenal manifestations include intracranial and aortic aneurysms and cystic disease of liver and pancreas (8–11). The biological functions of PC1 are poorly defined in some tissues that express *PKD1* transcripts, such as bone. Indeed, the absence of clinically demonstrable skeletal abnormalities in patients with ADPKD initially delayed the investigation of PKD1 function in bone. The apparent lack of abnormalities in other tissues expressing PC1 may arise because of differences in the frequency of a second hit somatic mutation, the presence of other modifying factors that may compensate for lack of PC1 function in other organs (12), or failure to detect more subtle phenotypes. For example, lung was not thought to be affected by *PKD1* mutations until computed tomography scans of lungs of ADPKD patients showed a 3-fold increase in the prevalence of bronchiectasis compared with controls (13).

Pkd1 is highly expressed in bone, and several mouse models with inactivating mutations of *Pkd1* have skeletal abnormalities in the setting of polycystic kidney disease and embryonic lethality (6, 7, 14–16). Most recently, however, the heterozygous *Pkd1*^{m1Bei} mouse, which has an inactivating mutation of *Pkd1* and survives to adulthood without polycystic kidney disease, has been shown to develop osteopenia and impaired osteoblastic differentiation (17, 18), suggesting that *Pkd1* may function in bone. Because homozygous *PKD1*/*Pkd1* mutations in humans and mice are lethal, and most of the existing models are globally *Pkd1*-deficient, the significance of inactivation of *Pkd1* in osteoblasts remains uncertain, and the bone changes might reflect an indirect effect due to loss of PKD1, in the kidney or other tissues.

In the current study, to determine if PKD1 in osteoblasts has a direct function in regulating postnatal skeletal functions, we used mouse genetic approaches to conditionally delete *Pkd1* in osteoblasts. We demonstrate that conditional deletion of *Pkd1* from osteoblasts using *Oc*-Cre results defective osteoblast function *in vivo* and *in vitro*, and osteopenia, indicating that PKD1 has a direct role to regulate osteoblast function and skeletal homeostasis.

EXPERIMENTAL PROCEDURES

Mice—We obtained the floxed *Pkd1* mice from Dr. Gregory Germino at Johns Hopkins University (19) and *Oc* (osteocalcin)-Cre mice from Dr. Thomas Clemens at the University of Alabama (20). The *Pkd1*^{m1Bei} heterozygous mice were available in our laboratory as described previously (18). These mice were

* This work was supported, in whole or in part, by National Institutes of Health Grants R01-AR049712 and R21-AR056794.

[1] To whom correspondence should be addressed: University of Kansas Medical Center, MS 3018, 3901 Rainbow Blvd., 6018 Wahl Hall East, Kansas City, KS 66160. Tel.: 913-588-9252; Fax: 913-588-9251; E-mail: dquarles@kumc.edu.

[2] The abbreviations used are: ADPKD, autosomal dominant polycystic kidney disease; BMD, bone mineral density; μCT, microcomputed tomography; MAR, mineral apposition rate; MS/BS, mineralized surface per bone surface; BFR, bone formation rate; RT, reverse transcription; BisTris, 2-[bis(2-hydroxyethyl)amino]-2-(hydroxymethyl)propane-1,3-diol; PI3K, phosphatidylinositol 3-kinase.

bred and maintained on a C57BL/6J background. At first, we created double heterozygous *Oc*-Cre;*Pkd1*$^{m1Bei/+}$ mice and homozygous *Pkd1*$^{flox/flox}$ mice. Then double heterozygous *Oc*-Cre;*Pkd1*$^{m1Bei/+}$ mice were mated with homozygous *Pkd1*$^{flox/flox}$ mice to generate excised floxed *Pkd1* heterozygous (*Oc*-Cre;*Pkd1*$^{flox/+}$) and null mice (*Oc*-Cre;*Pkd1*$^{flox/m1Bei}$ or *Pkd1*$^{Oc\text{-}cko}$) as well as Beier *Pkd1* heterozygous mice (*Pkd1*$^{m1Bei/flox}$) and *Oc*-Cre negative control mice (*Pkd1*$^{flox/+}$, equivalent to wild type). These mice were used for phenotypic analysis. Animal experiments were performed, following review and approval by the University of Kansas Medical Center's Animal Care and Use Committee.

Genotyping PCR and Real-time PCR to Detect Mutations and Deletions—Genomic DNA was prepared from bone and other tissue specimens using standard procedures. PCR genotyping was performed using the following primers (19) (Fig. 1*A*): F1, 5′-CTT CTA TCG CCT TCT TGA CGA GTT C-3′; R1, 5′-AGG GCT TTT CTT GCT GGT CT-3′; R2, 5′-TCG TGT TCC CTT ACC AAC CCT C-3′. *Pkd1* floxed (*Pkd1*^{flox}) alleles were identified in 2% agarose gels as 670 bp bands (Fig. 1*B*). The Δ floxed *Pkd1* (*Pkd1*$^{\Delta flox}$) allele was detected as a 0.85 kb band in 1% agarose gels (Fig. 1*B*). The *Pkd1*^{m1Bei} allele was genotyped using SYBR® Green (Bio-Rad) real-time PCR as described previously (18).

Bone Densitometric, Histomorphometric, and Microcomputed Tomography (μCT) Analysis—Bone mineral density (BMD) of femurs was assessed at 16 weeks of age using a LUNAR$_{PIXIMUS}$ bone densitometer (Lunar Corp., Madison, WI). Calcein (Sigma) double labeling of bone and histomorphometric analyses of periosteal mineral apposition rate (MAR), mineralized surface per bone surface (MS/BS), and bone formation rate (BFR) in tibias were performed using the osteomeasure analysis system (Osteometrics). Goldner and Von Kossa staining were performed according to standard protocols (21, 22). The distal femoral metaphyses were also scanned using a Scanco μCT 40 (Scanco Medical AG, Brüttisellen, Switzerland). A three-dimensional image analysis was done to determine bone volume/total volume and cortical thickness as described previously (18, 21).

Detection of Bone Marrow Adipocytes in Long Bones by Oil Red O Lipid Staining—Whole intact femurs with encapsulated marrow were dissected from 18-week-old mice, fixed for 48 h in phosphate-buffered paraformaldehyde, decalcified in 14% EDTA, and then embedded in tissue freezing medium. Cryosectioning was performed on a Leica CM1900 cryostat (Leica, Nussloch, Germany) equipped with a CryoJane frozen sectioning kit (Instrumedics, Hackensack, NJ). 10-μm thick sections were then stained with Oil Red O for bone marrow adipocytes as described before (23). Briefly, the sections were rinsed in 60% isopropyl alcohol; stained for 20 min in 0.5% Oil Red O, isopropyl alcohol solution; differentiated in 60% isopropyl alcohol; rinsed in tap water; and mounted in glycerin jelly. Sections were examined with a Leica DM LB microscope equipped with an Optronics digital camera.

Detection of Bone Marrow Fat in Long Bones by μCT—Whole intact tibiae with encapsulated marrow were dissected from 18-week-old mice, fixed for 48 h in phosphate-buffered paraformaldehyde, decalcified in 14% EDTA, and stained for 2 h in 2% aqueous osmium tetroxide (OsO_4). Bones were rinsed in water for 48 h and then scanned at 6 μm resolution using a Scanco μCT 40, 45 keV, and 177 μA. Quantification of fat volume, density, and distribution throughout the marrow was registered to low contrast decalcified bone.

Real-time RT-PCR—For quantitative real-time RT-PCR, 2.0 μg of total RNA isolated from either the long bone of 16-week-old mice or 10-day cultured primary osteoblasts in differentiation medium was reverse transcribed as described previously (24). PCRs contained 100 ng of template (cDNA or RNA), 300 nM each forward and reverse primers, and 1× iQ™ SYBR® Green Supermix (Bio-Rad) in 50 μl. The threshold cycle of tested gene product from the indicated genotype was normalized to the threshold cycle for cyclophilin A. Expression of total *Pkd1* transcripts was performed using the following *Pkd1* allele-specific primers: in exon 26, forward primer of normal *Pkd1*$^{+}$ transcript (5′-CTG GTG ACC TAT GTG GTC AT-3′), forward primer of mutant *Pkd1*^{m1Bei} transcript (5′-CTG GTG ACC TAT GTG GTC AG-3′), and common reverse primer (5′-AGC CGG TCT TAA CAA GTA TTT C-3′); in exons 2–4, forward primer of normal *Pkd1*$^{+}$ transcript (5′-ATA GGG CTC CTG GTG AAC CT-3′) and reverse primer (5′-CCA CAG TTG CAC TCA AAT GG-3′). The normal *Pkd1*$^{+}$ *versus* cyclophilin A is normalized to the mean ratio of five control mice, which has been set to 1. The percentage of conditional deleted and mutant transcripts was calculated from the relative levels of the normal *Pkd1*$^{+}$ transcripts in different *Pkd1* exons (25).

Serum Biochemistry—Serum osteocalcin levels were measured using a mouse osteocalcin enzyme immunoassay kit (Biomedical Technologies Inc., Stoughton, MA). Serum urea nitrogen was determined using a serum urea nitrogen diagnostic kit from Pointe Scientific, Inc. Serum calcium was measured by the colorimetric cresolphthalein binding method, and phosphorus was measured by the phosphomolybdate-ascorbic acid method (Stanbio Laboratory, TX). Serum TRAP (tartrate-resistant acid phosphatase) was assayed with the enzyme-linked immunosorbent assay-based SBA Sciences mouseTRAP™ assay (Immunodiagnostic Systems, Fountain Hills, AZ).

Primary Osteoblast Culture for Proliferation, Differentiation, and Western Blot Analysis—Primary osteoblasts from newborn mouse calvarias were cultured in α-minimum essential medium containing 10% fetal bovine serum and 1% penicillin/streptomycin as described previously (24). Cell proliferation was detected by bromodeoxyuridine incorporation assays as the manufacturer describes (QIA58, Calbiochem). To induce differentiation, primary osteoblasts were plated at a density of 1×10^5 cells/well in a 6-well plate and grown for period of up to 21 days in α-minimum essential medium containing 10% fetal bovine serum supplemented with 5 mM β-glycerophosphate and 25 μg/ml ascorbic acid. Alkaline phosphatase activity and alizarin red-S histochemical staining for mineralization were performed as described previously (24). Total DNA content was measured with a PicoGreen® double-stranded DNA quantitation reagent and kit (Molecular Probes, Inc., Eugene, OR).

To examine the amounts of cytoplasmic Akt, GSK, and β-catenin, the cells were prepared using 1× passive lysis buffer for 30 min at 4 °C (Promega, Madison, WI) and centrifuged at 100,000 × *g* for 45 min at 4 °C. Protein concentrations of the

supernatant were determined with a Bio-Rad protein assay kit (Bio-Rad). Equal quantities of protein were subjected to NuPAGE™ 4–12% BisTris gel (Invitrogen) and were analyzed with standard Western blot protocols (horseradish peroxidase-conjugated secondary antibodies from Santa Cruz Biotechnology, Inc. (Santa Cruz, CA) and ECL from Amersham Biosciences). Antibodies against phospho-Akt (Ser-473), Akt, phospho-GSK (Ser-9), and GSK were from Cell Signaling Technology (Beverly, MA). Anti-β-catenin (sc-7199) and anti-β-actin (sc-47778) antibodies were from Santa Cruz Biotechnology, Inc.

Transient Transfection—Both MC3T3-E1 and primary osteoblasts were cultured in α-minimum essential medium containing 10% fetal bovine serum and 1% penicillin/streptomycin. To examine if PC1 regulates *Runx2*-P1 promoter activity by coupling with PI3K-Akt signaling, 1×10^6 MC3T3-E1 cells were transfected with either control expression vector (sIgφ) or gain-of-function PC1 C-tail construct (PC1-AT) along with the *Runx2*-P1 luciferase reporter (p0.42*Runx2*-P1-Luc) construct by electroporation using Cell Line Nucleofector Kit R according to the manufacturer's protocol (Amaxa Inc., Gaithersburg, MD). A total of 10.2 μg of plasmid DNA was used for each electroporation, with 3.6 μg of PC1 C-tail construct, 2.4 μg of p0.42*Runx2*-P1-Luc reporter, the indicated amounts of a dominant negative *Akt* (dn-*Akt*) construct in combination with empty vector (3.6 μg), and 0.6 μg of *Renilla* luciferase-null (RL-null) as internal control plasmid. Promoter activity was assessed by measuring luciferase activity 48 h after transfection in the presence or absence of a PI3K inhibitor (0.1–10 μM; LY294002) and a dn-*Akt* construct (1.2–3.6 μg) as described previously (17, 18).

To explore potential abnormalities of the WNT pathway in excised floxed *Pkd1* null mice, control ($Pkd1^{flox/+}$) and excised floxed *Pkd1* null ($Pkd1^{Oc\text{-}cko}$) osteoblasts were transiently cotransfected with either pTOPFLASH or pFOPFLASH along with *Renilla* luciferase-null (RL-null; Promega, Madison, WI) as an internal control as described above. Promoter activity will be assessed by measuring luciferase activity 48 h after transfection in the presence or absence of 100 ng/ml recombinant Wnt3a treatment for the last 8 h.

Statistics—We evaluated differences between groups by one-way analysis of variance. All values are expressed as means ± S.D. All computations were performed using GraphPad Prism5 (GraphPad Software, Inc., La Jolla, CA).

RESULTS

Oc-Cre-mediated Bone-specific Deletion of Pkd1—The four genotypes from the breeding strategy (*Oc*-Cre;$Pkd1^{flox/m1Bei}$ or $Pkd1^{Oc\text{-}cKO}$, *Oc*-Cre;$Pkd1^{flox/+}$, $Pkd1^{flox/m1Bei}$, and $Pkd1^{flox/+}$) were born at the expected Mendelian frequency, and all exhibited survival indistinguishable from that of wild-type mice. The normal survival of conditional $Pkd1^{Oc\text{-}cKO}$ null mice (*Oc*-Cre;$Pkd1^{flox/m1Bei}$) contrasts with perinatal lethality of homozygous $Pkd1^{m1Bei/m1Bei}$ mice (17). *Oc*-Cre expression is limited to cells of the osteoblast lineage (late osteoblasts > osteocytes) with onset of expression just before birth and persisting throughout the mature osteoblast lineage (20). To confirm that the *Pkd1* floxed allele was selectively deleted in bone, we performed PCR analysis using a combination of primers that specifically detect floxed *Pkd1* alleles ($Pkd1^{flox}$) and the excised floxed *Pkd1* alleles ($Pkd1^{\Delta flox}$) in *Oc*-Cre;$Pkd1^{flox/+}$ or *Oc*-Cre;$Pkd1^{flox/m1Bei}$ mice (Fig. 1*A*). We demonstrated that *Oc*-Cre-mediated floxed recombination occurred exclusively in tissues that contain osteoblastic cells, whereas non-skeletal tissues retained the intact floxed *Pkd1* alleles ($Pkd1^{flox}$) (Fig. 1*B*). The $Pkd1^{m1Bei}$ mutation, which functions as a null allele, was used in combination with the floxed *Pkd1* allele ($Pkd1^{flox}$) to increase the net efficiency of *Pkd1* inactivation by Cre-recombinase to reduce functional *Pkd1* expression. Therefore, we examined the percentage of *Pkd1* conditional deleted and the $Pkd1^{m1Bei}$ mutant alleles in bone. The level of conditional deleted $Pkd1^{\Delta flox}$ alleles and the presence of the $Pkd1^{m1Bei}$ mutation from the femurs of these four genotypes of mice were assessed by real time PCR (Fig. 1*C*). Both $Pkd1^{flox/m1Bei}$ and *Oc*-Cre;$Pkd1^{flox/m1Bei}$ mice expressed 50% of the $Pkd1^{m1Bei}$ mutant allele, whereas *Oc*-Cre;$Pkd1^{flox/+}$ and *Oc*-Cre;$Pkd1^{flox/m1Bei}$ mice exhibited ~25% excision of the floxed exons 2–4 from *Pkd1*, indicating that *Oc*-Cre-mediated bone-specific deletion of the floxed *Pkd1* allele *is* incomplete (Fig. 1*C*). The combined effect of $Pkd1^{m1Bei}$ and ($Pkd1^{\Delta flox}$) in *Oc*-Cre;$Pkd1^{flox/m1Bei}$ resulted in a net reduction of *Pkd1* expression by ~75% in bone (Fig. 1*C*). Real-time RT-PCR to assess the level of expression of the residual functional *Pkd1* transcript confirmed the progressive reduction of functional *Pkd1* message in conditional mutant mice (*i.e.* $Pkd1^{flox/+}$ (100%), *Oc*-Cre;$Pkd1^{flox/+}$ (76%), $Pkd1^{flox/m1Bei}$ (50%), and *Oc*-Cre;$Pkd1^{flox/m1Bei}$ (25%) mice) (data not shown). In addition, *Oc*-Cre;$Pkd1^{flox/m1Bei}$ mice heterozygous for the conditional deleted $Pkd1^{\Delta flox}$ allele and mutant $Pkd1^{m1Bei}$ allele demonstrated no cyst formation in the kidney, consistent with the bone-specific inactivation of *Pkd1* (Fig. 1*D*). In contrast, positive control mice lacking *Pkd1* in the kidney have massive cyst formation in the kidney (Fig. 1*D*).

Additive Effects of Global Mutant ($Pkd1^{m1Bei}$) and Conditional Deleted ($Pkd1^{\Delta flox}$) Pkd1 Alleles Suggest a Direct Role for PKD1 in Bone—At 16 weeks of age, the gross appearance and body weight of single global and conditional heterozygous ($Pkd1^{flox/m1Bei}$ or *Oc*-Cre;$Pkd1^{flox/+}$) and control ($Pkd1^{flox/+}$) mice were not significantly different. The global *Pkd1* heterozygous mice ($Pkd1^{flox/m1Bei}$) and heterozygous conditional deleted *Pkd1* mice (*Oc*-Cre;$Pkd1^{flox/+}$), however, were osteopenic, as evidenced by respective 9 and 7% reduction BMD in both male and female adult mice (Fig. 2*A*). The phenotype of the $Pkd1^{Oc\text{-}cKO}$ mice was more severe. The body weight of both male and female $Pkd1^{Oc\text{-}cKO}$ mice was reduced by ~16 and 12% (data not shown) compared with the control mice ($Pkd1^{flox/+}$). In addition, $Pkd1^{Oc\text{-}cKO}$ mice had greater loss in BMD, with respective reductions in BMD of 14 and 13% reduction in male and female adult mice (Fig. 2*A*). The abnormalities in BMD in the various groups, although present at 6 weeks of age, segregated by gene dose by 16 weeks of age (Fig. 2*B*).

μCT analysis revealed that the reduction in bone mass in heterozygous *Pkd1*-deficient mice (either $Pkd1^{flox/m1Bei}$ or *Oc*-Cre;$Pkd1^{flox/+}$) was caused by a reduction in trabecular bone volume (24.3 and 25.5%, respectively) and cortical bone thickness (9.7 and 10.8%, respectively) (Fig. 2*C*). $Pkd1^{cKO/m1Bei}$

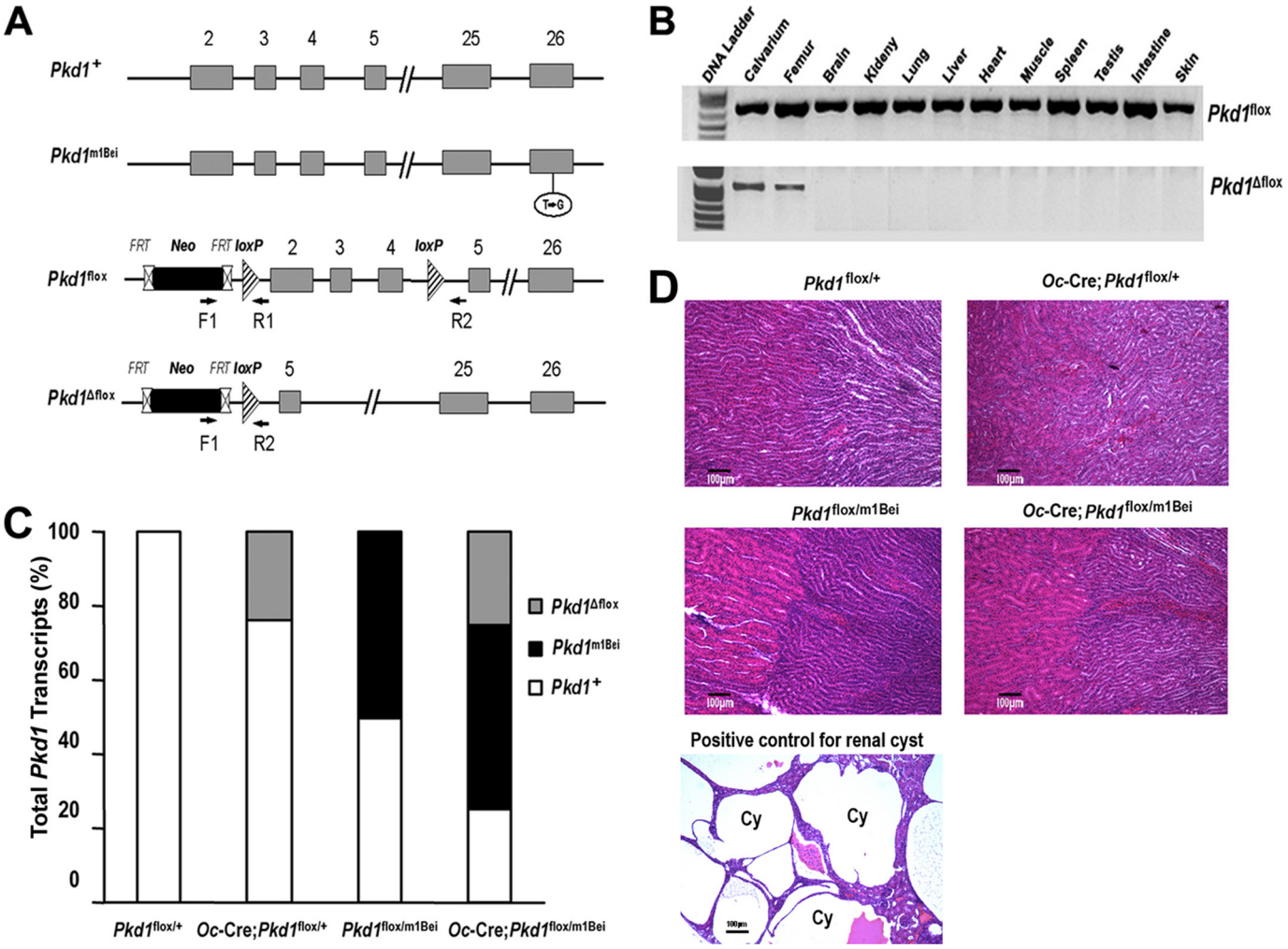

FIGURE 1. ***Oc*-Cre-mediated bone specific deletion of *Pkd1* from the floxed *Pkd1* allele (*Pkd1*^{flox}).** *A*, schematic illustration of wild-type (*Pkd1*$^{+}$), mutant (*Pkd1*^{m1Bei}), and floxed *Pkd1* allele before (*Pkd1*^{flox}) and after deletion (*Pkd1*$^{\Delta flox}$) of the lox P cassette containing exons 2–4 via Cre-mediated recombination. *B*, genotype PCR analysis of different tissues that were harvested from 16-week-old *Oc*-Cre;*Pkd1*$^{flox/m1Bei}$ mice showed bone-specific deletion of the *Pkd1* gene. *Osteocalcin*-Cre-mediated recombination of excised floxed *Pkd1* (*Pkd1*$^{\Delta flox}$) allele occurred exclusively in bone, whereas non-skeletal tissues retained the floxed *Pkd1* allele (*Pkd1*^{flox}). *C*, real-time RT-PCR analysis of total *Pkd1* transcripts. Data are expressed as the percentage expression of wild-type (*Pkd1*$^{+}$ and *Pkd1*^{flox}), mutant (*Pkd1*^{m1Bei}), and conditional deleted (*Pkd1*$^{\Delta flox}$) *Pkd1* alleles for each genotype from 5–6 tibias of 16-week-old mice. Expression of total *Pkd1* transcripts was performed using *Pkd1*-allele-specific primers as described under "Experimental Procedures." The normal *Pkd1*$^{+}$ *versus* cyclophilin A is normalized to the mean ratio of five control mice, which has been set to 1. The percentage of conditional deleted and mutant transcripts was calculated from the relative levels of the normal *Pkd1*$^{+}$ transcripts in different *Pkd1* exons. *D*, histology of adult kidney. Hematoxylin-eosin-stained sections from 16-week-old mice failed to identify any cystic tubules in either cortical or medullary regions of kidney from *Oc*-Cre;*Pkd1*$^{flox/+}$ or *Pkd1*$^{Oc\text{-}cko}$ mice, consistent with the absence of *Oc*-Cre expression in the kidney. In contrast, ablation of *Pkd1* in the kidney caused massive cyst formation, which served as a positive control. *Cy*, cyst. *Scale bars*, 100 μm.

had greater loss in both trabecular (44.5%) and cortical bone (21.0%) than did single heterozygous mice (Fig. 2*C*).

Consistent with a low bone mass phenotype by BMD and μCT analysis, both Goldner staining in distal femur and Von Kossa staining in vertebrae confirmed marked reductions in bone volume and cortical thickness in *Pkd1*$^{Oc\text{-}cKO}$ null mice (Fig. 3*A*). In addition, we found that bone loss was associated with a significant *Pkd1* gene dose-dependent decrease in periosteal MAR, MS/BS, and BFR. In this regard, MAR, MS/BS, and BFR were reduced by ~36%, ~33%, and ~57% in heterozygous *Pkd1*$^{flox/m1Bei}$ and *Oc*-Cre;*Pkd1*$^{flox/+}$ mice and ~65, ~60, and ~87% in *Pkd1*$^{Oc\text{-}cKO}$ null mice compared with age-matched controls, respectively (Fig. 3*B*).

To investigate the effects of *Pkd1* deficiency on gene expression profiles in bone, we examined by real-time RT-PCR the expression levels of a panel of osteoblast lineage-, osteoclast-, and chondrocyte-related mRNAs from the femurs of 16-week-old control, heterozygous *Pkd1*-deficient (*Oc*-Cre;*Pkd1*$^{flox/+}$ and *Pkd1*$^{m1Bei/+}$), and *Oc*-Cre;*Pkd1*$^{flox/m1Bei}$ mice (Table 1). Bone derived from heterozygous *Oc*-Cre;*Pkd1*$^{flox/+}$ and *Pkd1*$^{m1Bei/+}$ mice had measurable reductions in the osteoblast lineage gene transcripts, including *Runx2*-II, total *Runx2*, osteocalcin, osteopontin, *Bsp* (bone sialoprotein), *Opg* (osteoprotegerin), *RankL* (*Rank* ligand), *Dmp1* (dentin matrix protein 1), and *Phex* (phosphate-regulating gene with homologies to endopeptidases on the X chromosome) mRNA levels compared with control mice. Significantly greater reductions of *Runx2*-II, total *Runx2*, osteocalcin, osteopontin, *Bsp*, *RankL*, *and Dmp1* were observed in *Pkd1*$^{Oc\text{-}cKO}$ null mice. In this regard, the *Opg*/*RankL* expression ratio was increased in a gene dose-dependent manner (Table 1). Consistent with a ratio of Opg/*RankL* that favors the reduced osteoclastogenesis, bone expression of *Trap*

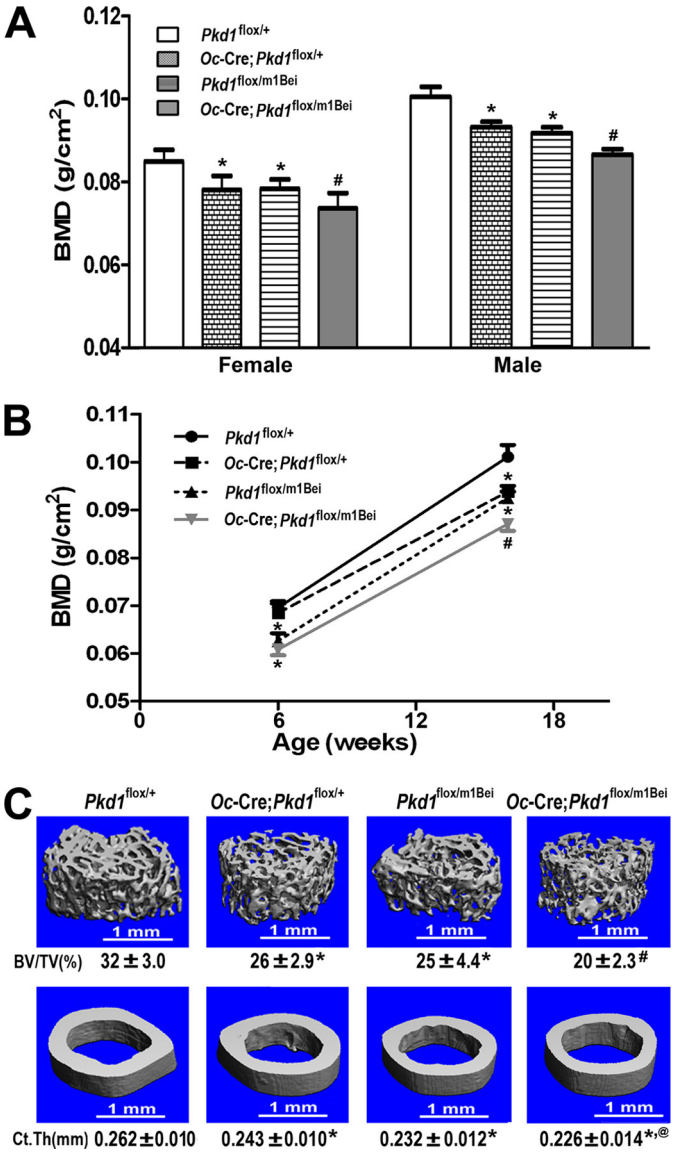

FIGURE 2. **Cre-mediated somatic loss of *Pkd1* results in loss of bone mass.** *A*, effects of $Pkd1^{\Delta flox}$ allele on BMD at 16 weeks of age. Similar to Beier *Pkd1* heterozygous mice ($Pkd1^{m1Bei/+}$), there was ~7–9% reduction in both male and female of BMD in single excised floxed *Pkd1* heterozygous mice (*Oc*-Cre; $Pkd1^{flox/+}$) compared with age-matched control mice ($Pkd1^{flox/+}$), and an even greater reduction (13–14%) in double heterozygous *Oc*-Cre;$Pkd1^{flox/m1Bei}$ ($Pkd1^{Oc\text{-}cko}$) mice, indicating an additive effect of global mutant and conditional deleted *Pkd1* alleles on loss of bone mass. *B*, age-dependent effects of $Pkd1^{\Delta flox}$ allele on BMD. Double heterozygous $Pkd1^{Oc\text{-}cko}$ mice displayed a significant decrease in femur BMD compared with $Pkd1^{m1Bei/+}$ mice until 16 weeks of age but not at 6 weeks of age, indicating an age-dependent effect of $Pkd1^{\Delta flox}$ allele on bone mass. *C*, effects of $Pkd1^{\Delta flox}$ allele on bone structure of femurs and midshaft diaphyses. μCT analysis of the distal femoral metaphyses and midshaft diaphyses revealed that double heterozygous $Pkd1^{Oc\text{-}cko}$ mice had greater loss in both trabecular and cortical bone than single *Oc*-Cre; $Pkd1^{flox/+}$ and $Pkd1^{m1Bei/+}$ heterozygous mice, consistent with additive effects of global mutant and conditional deleted *Pkd1* alleles on bone structure and a direct role of Pkd1 in bone. Data represent the mean ± S.D. from 8–10 individual mice. *, significant difference from control ($Pkd1^{flox/+}$); @, significant difference from single heterozygous *Oc*-Cre;$Pkd1^{flox/+}$; #, significant difference from single heterozygous *Oc*-Cre;$Pkd1^{flox/+}$ and $Pkd1^{flox/m1Bei}$ mice at $p < 0.05$, respectively.

and *Mmp9* (matrix metalloproteinase 9), markers of bone resorption, were also reduced in heterozygous *Pkd1*-deficient mice and to a greater extent in $Pkd1^{Oc\text{-}cKO}$ null mice (Table 1). Transcripts of chondrocyte-related genes did not differ between heterozygous *Pkd1*-deficient and $Pkd1^{Oc\text{-}cKO}$ null mice (Table 1).

Changes in gene expression in bone correlated with alterations in serum biomarkers. In this regard, further evidence for osteoblast dysfunction includes a reduction in osteocalcin in serum from 16-week-old heterozygous *Oc*-Cre;$Pkd1^{flox/+}$ and $Pkd1^{m1Bei/+}$ mice (Table 2). Serum levels of TRAP, a marker of bone resorption, were also reduced in heterozygous *Pkd1*-deficient mice compared with control littermates (Table 2). As with other parameters, $Pkd1^{Oc\text{-}cKO}$ null mice had greater reductions in bone formation and resorption markers, indicating additive effects of inactivation of both *Pkd1* alleles in bone homeostasis. Collectively, these findings suggest that *Pkd1*-mediated bone loss results from low bone formation rates rather than increased bone resorption (Fig. 2, *A–C*, and Table 2).

PPARγ (peroxisome proliferator-activated receptor γ), an adipocyte transcription factor, and adipocyte markers, including *Lpl* (lipoprotein lipase) and *aP2* (adipocyte fatty acid-binding protein 2) were increased femurs of *Pkd1*-deficient mice in a *Pkd1* gene dosage-related manner (Table 1). Consistent with increased adipogenic markers, bone marrow exhibited an increased percentage of fat cells in $Pkd1^{Oc\text{-}cKO}$ mice, as evidenced by a higher number of adipocytes and volume of fat droplets in decalcified femurs and tibias stained with Oil Red O and OsO_4 (Fig. 3*C*). In addition, the inflammatory cytokine *IFNγ* (interferon-γ) level, but not *TNFα* (tumor necrosis factor-α) and *TRAIL* (TNF-related apoptosis-inducing ligand) expression levels, was significantly elevated in *Pkd1*-deficient mice (Table 1). Moreover, *Alox15* (arachidonate 15-lipoxygenase) was also markedly increased in conditional *Pkd1*-deficient mice.

Effect of Conditional Deletion of Pkd1 on Osteoblastic Function ex Vivo—To determine the impact of conditional deleted *Pkd1* on osteoblast function *ex vivo*, we examined cell proliferation and osteoblastic differentiation and gene expression profiles in primary osteoblast cultures derived from control and $Pkd1^{Oc\text{-}cKO}$ null mice. Consistent with defects in bone formation, we found that $Pkd1^{Oc\text{-}cKO}$ null osteoblasts had a higher bromodeoxyuridine incorporation than control osteoblasts, indicating a greater proliferation rate in $Pkd1^{Oc\text{-}cKO}$ null osteoblasts (Fig. 4*A*). In addition, conditional null osteoblasts displayed impaired osteoblastic differentiation and maturation, as evidenced by lower alkaline phosphatase activity, diminished calcium deposition in extracellular matrix, and reduced osteoblastic differentiation markers compared with controls (Fig. 4, *B–D*). In agreement with increased adipogenic activity *in vivo*, the cultured primary calvarial cells under osteogenic conditions exhibited a marked increase of adipocyte markers, including *PPARγ*, *aP2*, and *Lpl* (Fig. 4*E*), suggesting impairment of osteogenesis and enhancement of adipogenesis in $Pkd1^{Oc\text{-}cKO}$ null osteoblast cultures.

Effect of Conditional Deletion of Pkd1 on PI3K-Akt-GSK-β-Catenin Signaling Pathway in Osteoblasts—PC1 encoded by *Pkd1* is coupled to multiple signal transduction pathways, including activation of canonical WNT/β-catenin and Akt-dependent pathways. There is evidence that Akt-dependent serine 9 phosphorylation of GSK3β prevents phosphorylation and degradation of β-catenin (26–29). Because the PI3K/Akt path-

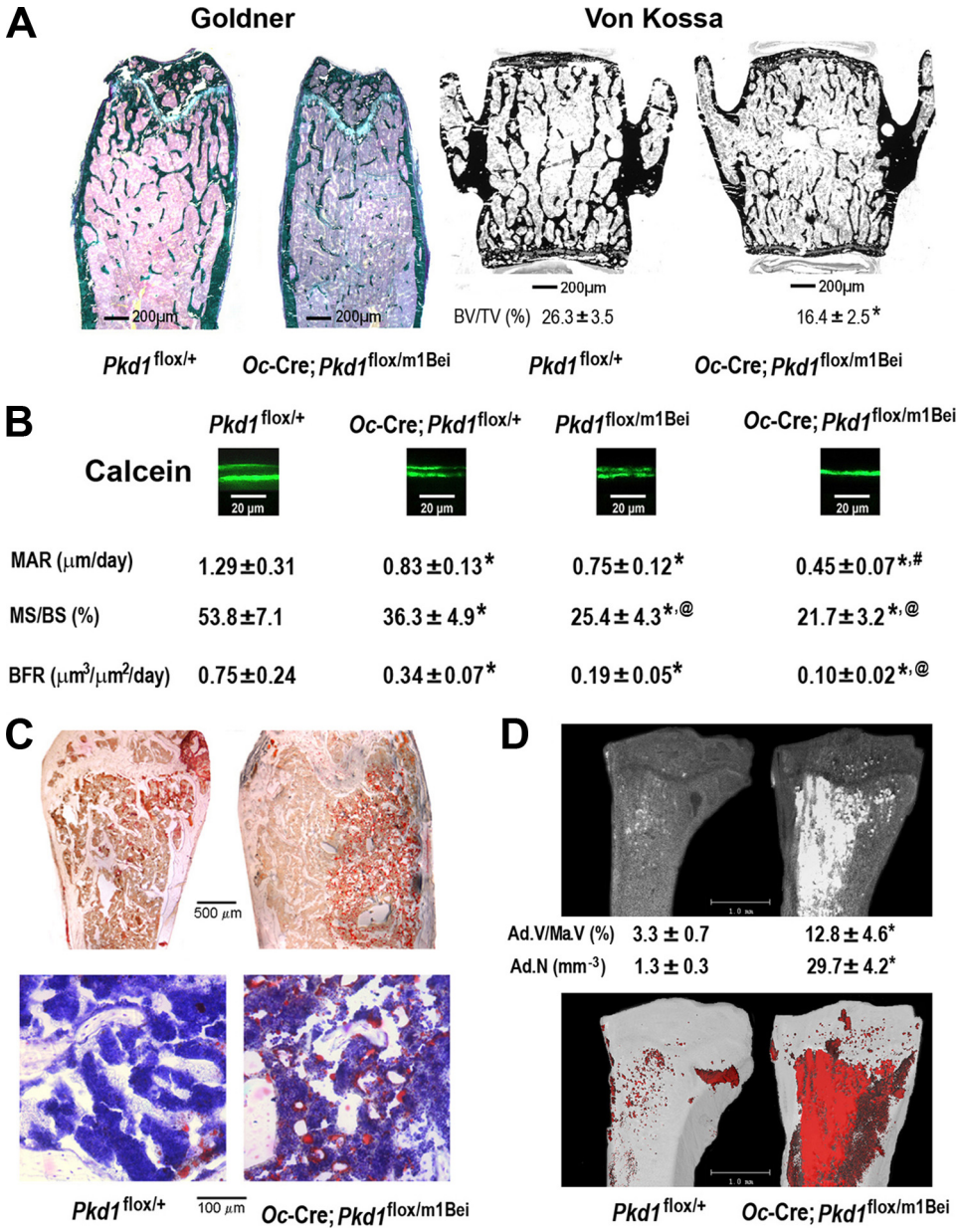

FIGURE 3. **Histological analysis of *Pkd1*$^{Oc\text{-}cKO}$ mice in bone.** *A*, Goldner and von Kossa staining of non-decalcified bone. Representative images of distal femur and lumbar vertebrate sections displayed markedly reductions in trabecular bone volume from 16-week-old *Pkd1*$^{Oc\text{-}cko}$ mice compared with age-matched control mice. *Scale bars*, 200 μm. *B*, bone histomorphometric analyses. There was a significant reduction in periosteal MAR, MS/BS, and BFR in single *Oc*-Cre;*Pkd1*$^{flox/+}$ and *Pkd1*$^{m1Bei/+}$ heterozygous mice compared with age-matched control *Pkd1*$^{flox/+}$ mice and an even greater decrement in double heterozygous *Pkd1*$^{Oc\text{-}cko}$ mice, indicating an additive effect of both global and conditional *Pkd1* deficiency to impair osteoblast-mediated bone formation. Representative images of the distal tibia-fibula junction sections from 16-week-old mice for each genotype showed progressive reductions in the distance between the two calcein labels (*scale bars*, 20 μm). *C*, Oil Red O staining of decalcified femur sections. Representative images of femoral bone marrow showed that the numbers of adipocytes and fat droplets were greater in 18-week-old *Pkd1*$^{Oc\text{-}cko}$ mice compared with age-matched control mice. *Scale bars*, 100 and 500 μm. *D*, OsO_4 staining of decalcified tibias by μCT analyses. Qualitatively, the images of osmium staining (*white* or *red areas*) were much higher in the proximal tibia from 18-week-old *Pkd1*$^{Oc\text{-}cko}$ mice compared with age-matched control mice. Quantifications of fat cell number and volume were also performed as described under "Experimental Procedures." *Ad.V/Ma.V* (%), adipocyte volume/marrow volume; *Ad.N* (mm^{-3}), adipocyte number (mm^{-3}). *Scale bars*, 1.0 mm. Data are mean ± S.D. from 3–5 individual mice. *, significant difference from control (*Pkd1*$^{flox/+}$); @, significant difference from single heterozygous *Oc*-Cre;*Pkd1*$^{flox/+}$; #, significant difference from single heterozygous *Oc*-Cre;*Pkd1*$^{flox/+}$ and *Pkd1*$^{flox/m1Bei}$ mice at $p < 0.05$, respectively.

way and WNT signaling play a role in osteoblastic development (30, 31), we determined the level of Akt phosphorylation in *Pkd1*$^{Oc\text{-}cKO}$ derived osteoblasts. Basal phospho-Akt relative to total Akt expression and phosphorylation of serine 9 of GSK3β were reduced in *Pkd1*$^{Oc\text{-}cKO}$ null osteoblasts compared with controls. To determine if potential cross-talk between the PC1/PI3K/Akt pathway and the WNT/GSK3β/β-catenin pathways have functional consequences (28), we next examined the response of osteoblasts derived from *Pkd1*$^{Oc\text{-}cKO}$ mice to Wnt3a. *Pkd1*$^{Oc\text{-}cKO}$-derived osteoblasts had a reduced response to Wnt3a-mediated phosphorylation of Akt when compared with control cells (Fig. 5*A*). In contrast, the addition of Wnt3a resulted in an increase in phosphorylation of GSK3β in control cells, leading to the inactivation of GSK3β (Fig. 5*A*). To determine if inhibition of GSK3β activated β-catenin (32), we assessed the accumulation of free β-catenin in the cytoplasm (33). Consistent with reduction of GSK3β phosphorylation, we found that the basal level of cytosolic β-catenin was lower in *Pkd1*$^{Oc\text{-}cKO}$ null osteoblasts and exhibited no increase following Wnt3a treatment, whereas control cells increased cytoplasmic β-catenin levels following Wnt3a stimulation (Fig. 5*A*).

To examine the effect of *Pkd1* inactivation on Wnt/β-catenin transcriptional activity, we examined TOPFlash activity in *Pkd1*$^{Oc\text{-}cKO}$ null osteoblasts. We observed a significant reduction of basal TOPFLASH activity in primary osteoblasts derived from *Pkd1*$^{Oc\text{-}cko}$ mice compared with the controls. In addition, Wnt3a-induced TOPFLASH activity was more than 2-fold above basal level in the control osteoblasts, whereas Wnt3a-induced TOPFLASH activity was only 1.4-fold above basal level in the *Pkd1*$^{Oc\text{-}cKO}$ null mice (Fig. 5*B*), indicating that loss of PC1 significantly attenuates responsiveness of the Wnt/β-catenin pathway in osteoblasts.

To examine the role of PC1-dependent Akt activation on transcriptional control of osteoblast development, we examined *Runx2*-II promoter activity. In previous studies, we have shown that PC1 is coupled to *Runx2*-II expression, a master regulator

TABLE 1

Gene expression profiles in 16-week-old mice

Data are mean ± S.D. from 5–6 tibias of 6-week-old individual mice and expressed as the -fold changes relative to the housekeeping gene cyclophilin A subsequently normalized to control (*Pkd1*$^{flox/+}$) mice.

Gene	Accession no.	*Oc*-Cre;*Pkd1*$^{flox/+}$	*Pkd1*$^{flox/m1Bei}$	*Oc*-Cre;*Pkd1*$^{flox/m1Bei}$	*p* value
Osteoblast lineage					
Runx2-II	NM_009820	0.73 ± 0.04[a]	0.71 ± 0.08[a]	0.45 ± 0.07[a,b]	0.0007
Runx2-I	D14636	1.14 ± 0.32	1.16 ± 0.14	1.15 ± 0.18	0.5961
Runx2	NM_009820	0.73 ± 0.09[a]	0.71 ± 0.16[a]	0.51 ± 0.07[a,b]	0.0009
Osteocalcin	NM_007541	0.82 ± 0.12[a]	0.80 ± 0.11[a]	0.46 ± 0.08[a,b]	<0.0001
Osteopontin	AF515708	0.73 ± 0.11[a]	0.69 ± 0.11[a]	0.44 ± 0.03[a,b]	0.0027
Bsp	NM_008318	0.73 ± 0.07[a]	0.71 ± 0.08[a]	0.52 ± 0.06[a,b]	<0.0001
Opg	MMU94331	0.71 ± 0.15[a]	0.70 ± 0.11[a]	0.68 ± 0.20[a]	0.0295
Rank ligand	NM_011613	0.70 ± 0.12[a]	0.57 ± 0.07[a]	0.39 ± 0.07[a,b]	<0.0001
Mmp13	NM_008607	0.97 ± 0.16	0.65 ± 0.05[a]	0.43 ± 0.11[a,b]	<0.0001
Dmp1	MMU242625	0.71 ± 0.06[a]	0.64 ± 0.12[a]	0.40 ± 0.05[a,b]	<0.0001
Phex	NM_011077	0.72 ± 0.12[a]	0.67 ± 0.12[a]	0.58 ± 0.14[a]	0.0002
Osteoclast					
Trap	NM_007388	0.68 ± 0.11[a]	0.63 ± 0.13[a]	0.36 ± 0.09[a,b]	<0.0001
Mmp9	NM_013599	0.95 ± 0.16	0.69 ± 0.08[a]	0.63 ± 0.07[a]	0.0001
Chondrocyte					
Collagen II	NM_031163	0.99 ± 0.13	1.03 ± 0.26	1.13 ± 0.23	0.5764
VegfA	NM_009505	1.07 ± 0.26	1.06 ± 0.21	0.97 ± 0.31	0.8905
Adipocyte					
PPARγ	NM_009505	1.08 ± 0.15	1.20 ± 0.19	1.40 ± 0.13[a]	0.0025
aP2	NM_024406	1.13 ± 0.16	1.55 ± 0.23[a]	1.95 ± 0.26[a,b]	<0.0001
Lpl	NM_008509	1.38 ± 0.25[a]	1.42 ± 0.27[a]	2.01 ± 0.29[a,b]	<0.0001
Others					
IFNγ	NM_008337	2.42 ± 0.79[a]	2.70 ± 1.21[a]	3.57 ± 1.51[a]	0.0039
TNFα	NM_013693	1.18 ± 0.32	1.23 ± 0.69	1.13 ± 0.39	0.8371
TRAIL	NM_009425	1.36 ± 0.51	1.33 ± 0.48	1.29 ± 0.45	0.4500
Alox15	NM_009660	1.93 ± 0.38[a]	2.22 ± 0.89[a]	2.40 ± 0.95[a]	0.0106

[a] Significant difference from control (*Pkd1*$^{flox/+}$) at $p < 0.05$.
[b] Significant difference from single heterozygous *Oc*-Cre;*Pkd1*$^{flox/+}$ and *Pkd1*$^{flox/m1Bei}$ mice at $p < 0.05$.

TABLE 2

Biochemistry analysis of serum in 16-week-old mice

Data are mean ± S.D. from nine individual mice. Osteocalcin is produced by osteoblasts, and TRAP is produced by osteoclasts.

Genotype	*Pkd1*$^{flox/+}$	*Oc*-Cre;*Pkd1*$^{flox/+}$	*Pkd1*$^{flox/m1Bei}$	*Oc*-Cre;*Pkd1*$^{flox/m1Bei}$
Serum urea nitrogen (mg/dl)	19 ± 4.9	20 ± 4.8	22 ± 4.3	22 ± 5.2
Calcium (mg/dl)	8.9 ± 0.27	8.7 ± 0.38	8.6 ± 0.34	8.5 ± 0.37
Phosphorus (mg/dl)	8.3 ± 0.95	8.5 ± 1.17	8.6 ± 1.50	8.8 ± 0.76
Osteocalcin (ng/ml)	87 ± 21.3	74 ± 13.8[a]	64 ± 18.6[a]	56 ± 12.6[a,b]
TRAP (units/liter)	12.6 ± 4.54	8.0 ± 2.94[a]	6.5 ± 1.61[a]	5.1 ± 0.94[a,b]

[a] Significant difference from control (Pkd1$^{flox/+}$) at $p < 0.05$.
[b] Significant difference from single heterozygous *Oc*-Cre;Pkd1$^{flox/+}$ and Pkd1$^{flox/m1Bei}$ mice at $p < 0.05$.

in osteoblast function, and that transfection of the C-terminal region of PC1 (PC1-AT) was sufficient to activate the *Runx2*-II P1 promoter/reporter construct (17). As shown in Fig. 5, *C* and *D*, we found that either the PI3K inhibitor LY294002 or cotransfection with a dn-*Akt* construct resulted in a dose-dependent inhibition of PC1-AT-mediated increase in *Runx2*-II P1 promoter activity.

Examination of Wnt-related gene expression in *Pkd1*$^{Oc\text{-}cKO}$ null osteoblasts further supports impairment of WNT/β-catenin signaling. In this regard, we found evidence for down-regulation of *Wnt10b*, *Axin2*, *Cox2*, and *Runx2*-II and up-regulation of the negative regulators *sFrp1* and *sFrp4* (Fig. 5*E*).

DISCUSSION

PC1 is expressed in cells within the osteoblast lineage (18), and skeletal abnormalities have been reported in *Pkd1* mutant mouse models (14, 15, 17, 18), but from these generalized loss-of-function observations it was not clear if the observed skeletal abnormalities were an indirect consequence of loss of PC1 in multiple tissues or a direct effect of loss of PC1 in osteoblasts. In the present studies, we have addressed this question by using *Oc*-Cre to conditionally inactivate *Pkd1* in mature osteoblasts postnatally. First, we have shown that the heterozygous conditional reduction of *Pkd1* in osteoblasts in *Oc*-Cre;*Pkd1*$^{flox/+}$ results in an osteopenic bone phenotype indistinguishable from the global *Pkd1*$^{flox/m1Bei}$ mice. The fact that *Oc*-Cre;*Pkd1*$^{flox/+}$ mice had a ~25% reduction in *Pkd1* expression, whereas *Pkd1*$^{flox/m1Bei}$ mice had a 50% reduction but had identical effects on bone, suggests that loss of *Pkd1* function in osteoblasts is responsible for the observed reduction in bone mass in both models. Moreover, the additive effects on the severity of osteopenia in combined conditional deletion of *Pkd1* in osteoblasts superimposed on the inactivated *Pkd1*^{m1Bei} allele in *Oc*-Cre;*Pkd1*$^{flox/m1Bei}$ (or *Pkd1*$^{Oc\text{-}cKO}$) mice, which resulted in ~2-fold greater (~14%) reduction in BMD associated with a 75% overall reduction in *Pkd1* expression in bone, compared with a 50% reduction in other tissues, indicates a dose-dependent function of *Pkd1* in mature osteoblasts.

We purposely did not create *Oc*-Cre;*Pkd1*$^{flox/flox}$ mice, due to the relative inefficiency of the *Oc*-Cre, which, based on the 25% reduction in *Pkd1* transcripts observed in *Oc*-Cre;*Pkd1*$^{flox/+}$ mice, may have only reduced expression in *Oc*-Cre;*Pkd1*$^{flox/flox}$

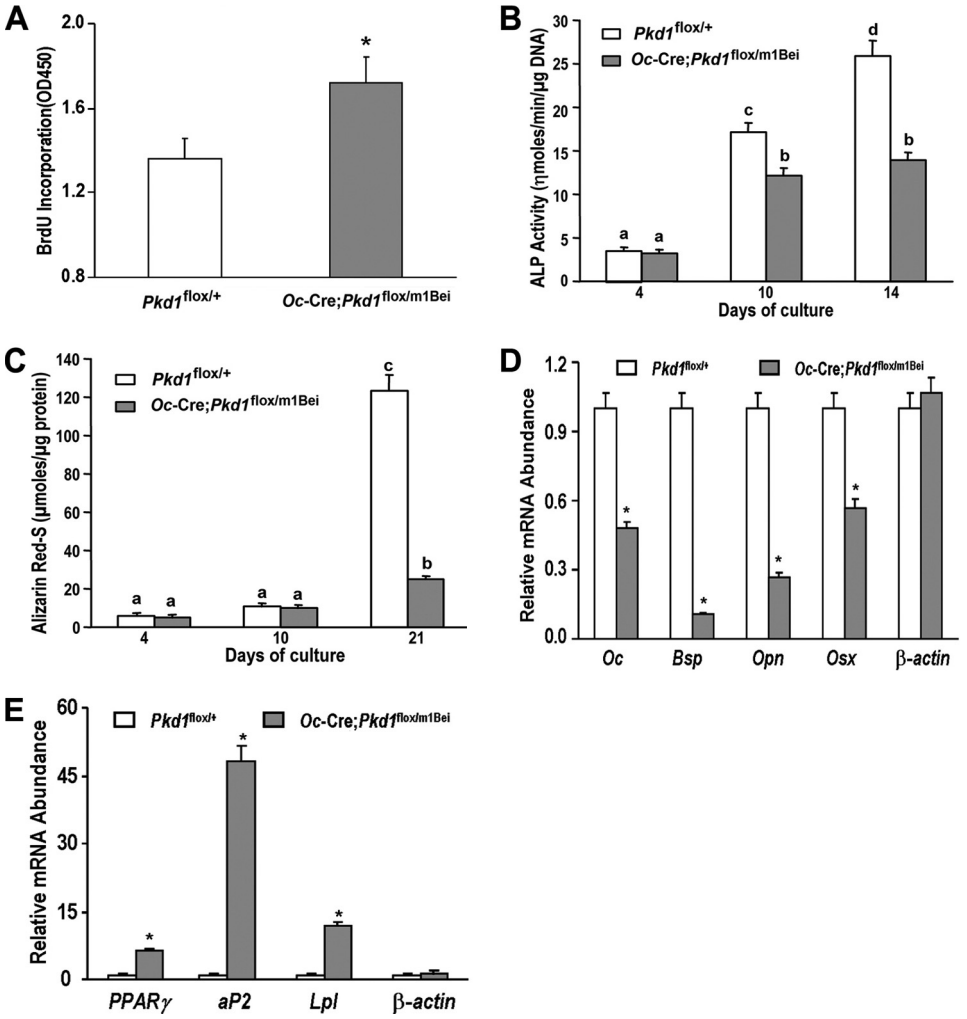

FIGURE 4. ***Pkd1*$^{Oc\text{-}cKO}$ osteoblasts have a developmental defect *ex vivo*.** *A*, bromodeoxyuridine (*BrdU*) incorporation. Primary cultured *Pkd1*$^{Oc\text{-}cKO}$ osteoblasts exhibited a higher bromodeoxyuridine incorporation than control *Pkd1*$^{flox/+}$ osteoblasts for 6 h, indicating increased proliferation in the *Pkd1*$^{Oc\text{-}cKO}$ osteoblasts. *B*, alkaline phosphatase (*ALP*) activity. Primary cultured *Pkd1*$^{Oc\text{-}cKO}$ osteoblasts displayed time-dependent increments in alkaline phosphatase activities for 14 days of culture, but the alkaline phosphatase activity was significantly lower at different time points compared with control *Pkd1*$^{flox/+}$ osteoblasts. *C*, quantification of mineralization. Alizarin Red-S was extracted with 10% cetylpyridinium chloride and quantified as described under "Experimental Procedures." Primary cultured *Pkd1*$^{Oc\text{-}cKO}$ osteoblasts had time-dependent increments in Alizarin Red-S accumulation for 21 days of culture, but the accumulation was significantly lower at different time points compared with control *Pkd1*$^{flox/+}$ osteoblasts. *D* and *E*, gene expression profiles by real-time RT-PCR. 10-day cultured *Pkd1*$^{Oc\text{-}cKO}$ osteoblasts in osteogenic differentiation medium showed a significant attenuation in osteogenesis compared with control osteoblasts, as evidenced by a significant reduction in osteoblastic markers, including osteocalcin (*Oc*), bone sialoprotein (*Bsp*), osteopontin (*Opn*), *and* osterix (*Osx*). However, a marked increase of adipocyte markers, such as *PPARγ*, *aP2*, and *Lpl*, was observed from the *Pkd1*$^{Oc\text{-}cKO}$ osteoblasts under the same differentiation medium when compared with control osteoblasts. Data are mean ± S.D. from triple three independent experiments. *, significant difference from control (*Pkd1*$^{flox/+}$) mice at $p < 0.05$. Values sharing the same *superscript* in *B* and *C* are not significantly different at $p < 0.05$.

mice to levels similar to the heterozygous *Pkd1*$^{flox/m1Bei}$ mice (*e.g.* 50%). Thus, to achieve greater reduction in *Pkd1* expression in osteoblasts (*e.g.* ~75%), we created *Oc*-Cre;*Pkd1*$^{flox/m1Bei}$ mice. It is of note that the magnitude of bone loss in *Pkd1*$^{Oc\text{-}cKO}$ mice is comparable with the 16% reduction in BMD found in Lrp5 null mice (34), a receptor known to have important anabolic osteoblast-mediated functions in bone through activation of canonical Wnt signaling pathways, and exceeds bone loss observed in oophorectomized mice (which is typically <10%) (35). Because *Pkd1*$^{Oc\text{-}cKO}$ had no demonstrable extraskeletal phenotypes and loss of *Pkd1* was greatest in bone, these findings are most consistent with a direct role of PC1 to regulate osteoblast function. Evidence for impaired osteoblastic function in *Pkd1*$^{Oc\text{-}cko}$ null mice is evident from both *in vivo* and *ex vivo* analysis. Bone from *Pkd1*$^{Oc\text{-}cko}$ null mice displayed decreased MAR, MS/BS, BFR, and reduced expression of osteoblastic markers, including the *Runx2*-II isoform, which regulates osteoblast development and function.

Ex vivo assessment of primary osteoblasts isolated confirmed an intrinsic impairment of osteoblast maturation as well as identified increased proliferation, which are typically inversely related (36). A feature of ADPKD renal cells is increased proliferation rate as well as impaired differentiation of epithelial cells (37); our findings suggest that this phenotypic switch may also occur in osteoblasts. Indeed, the *Pkd1*$^{Oc\text{-}cKO}$ null osteoblasts showed a greater proliferation rate as well as impaired osteoblastic differentiation and maturation. Because others have shown that the response of the renal epithelium to acquired loss of *Pkd1* is determined by the developmental state of the organ (38), our data showing a defect in osteoblast maturation in remodeling bone raises the possibility that *Pkd1* may also play a role in the embryogenesis of bone. Osteoblasts and adipocytes undergo renewal from bone marrow-derived precursors, and the ratio of osteoblasts and adipocytes appears to be reciprocally controlled in response to physiological stimuli and aging (39). We also found an inverse dose relationship between *Pkd1* expression and adipogenesis marker expression in the *Pkd1*$^{Oc\text{-}cKO}$ osteoblast cultures compared with the control. In agreement with this *in vitro* data, our *in vivo* study also showed strong evidence for lipid droplet accumulation in the bone marrow of *Pkd1*$^{Oc\text{-}cKO}$ mice compared with the control mice via Oil Red O and osmium staining. This phenomenon was also supported by an enhanced expression of inflammatory mediators, such as *IFNγ* and *Alox15* (40, 41), which, produced by adipose tissues, strongly suppress osteoblastogenesis. The findings of increased fat cells in bone marrow of *Pkd1*$^{Oc\text{-}cKO}$ mice and impaired development of osteoblast cultures derived from *Pkd1*$^{Oc\text{-}cKO}$ mice suggest that *Pkd1* deficiency may lead to impaired differentiation of mesenchymal stem

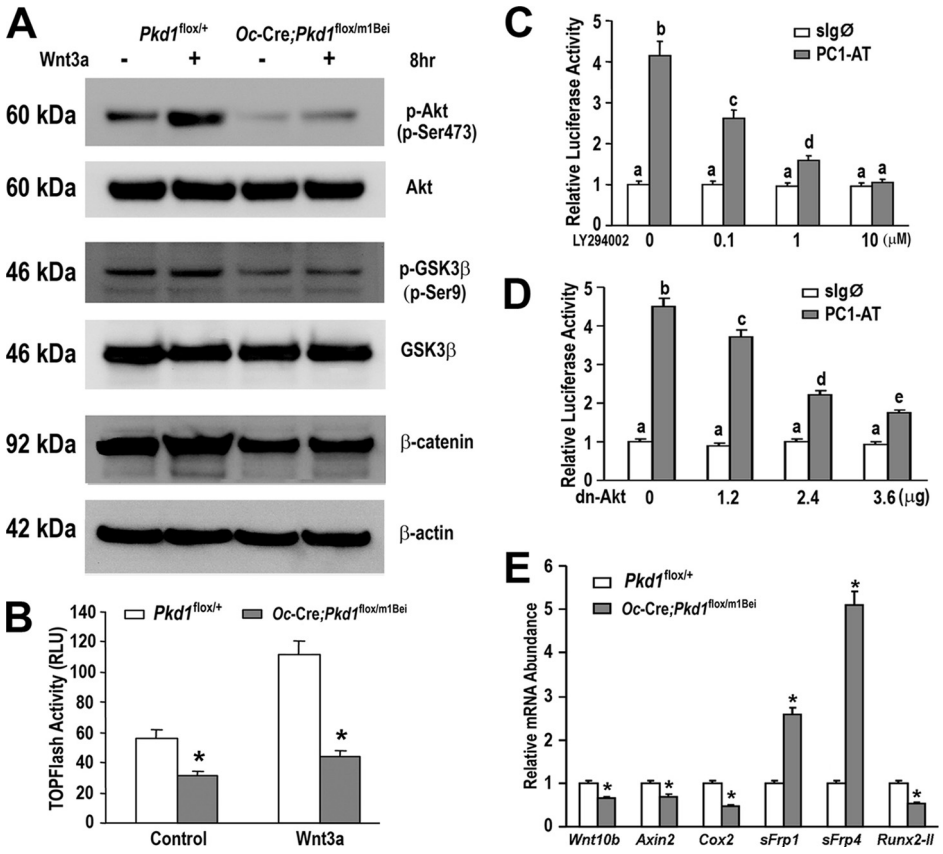

FIGURE 5. **Signaling pathways in *Pkd1*$^{Oc\text{-}cKO}$ osteoblasts.** *A*, Western blot analysis. Comparison of Akt, GSK3β, and β-catenin expressions in control and *Pkd1*$^{Oc\text{-}cKO}$ osteoblasts treated with or without Wnt3a (100 ng/ml) for the indicated times. Phosphorylated Akt at Ser-473 (*panel 1*) coincides with phosphorylation of GSK3β at Ser-9 (*panel 3*), reflecting its inactivation by Akt and followed by accumulation of cytoplasmic β-catenin, as detected by Western blot. Total Akt (*panel 4*), GSK3β (*panel 4*), and β-actin (*panel 6*) were used as loading controls for phospho-Akt, phospho-GSK3β, and β-catenin in the cytoplasm, respectively. *Pkd1*$^{Oc\text{-}cKO}$ osteoblasts exhibited suppressed activity of the PI3K-Akt-GSK3β-β-catenin signaling pathway under basal and Wnt3a-stimulated conditions. *B*, TCF/LEF-dependent transcriptional activation as assessed by pTOPFLASH activity. *Pkd1*$^{Oc\text{-}cKO}$ osteoblasts display lower levels of basal TCF/LEF-dependent reporter activity (TOPFLASH) when compared with control *Pkd1*$^{flox/+}$ osteoblasts. Wnt3a (100 ng/ml) induced reporter activity by more than 2.0-fold above control in *Pkd1*$^{flox/+}$ osteoblasts, whereas Wnt3a induced reporter activity by only 1.4-fold above control in *Pkd1*$^{Oc\text{-}cKO}$ osteoblasts. *C* and *D*, PC1-mediated regulation of *Runx2*-II-P1 prompter activity via the PI3K/Akt pathway. Wild-type MC3T3-E1 cells were transiently transfected either with control expression vector (slgφ) or gain-of-function PC1 C-tail construct (PC1-AT) along with the *Runx2*-II-P1 luciferase reporter (p0.42*Runx2*-P1-Luc) construct in the presence or absence of PI3K inhibitor LY294002 or dn-*Akt* construct. PC1-mediated activation of *Runx2*-II-P1 promoter activity was dose-dependently diminished by either PI3K inhibitor LY294002 or dn-*Akt* construct. *E*, gene expression profiles by real-time RT-PCR. 10-day cultured *Pkd1*$^{Oc\text{-}cKO}$ osteoblasts in differentiation medium showed a significant attenuation in WNT/β-catenin signaling compared with control osteoblasts, as evidenced by a significant down-regulation of WNT/β-catenin-targeting genes, including *Wnt10b*, *Axin2*, *Cox2*, and *Runx2*-II, and up-regulation of its antagonist genes, such as *sFrp1* and *sFrp4*. Data are mean ± S.D. from triple independent experiments. *, significant difference from control (*Pkd1*$^{flox/+}$) mice at $p < 0.05$. Values sharing the same *superscript* in *C* and *D* are not significantly different at $p < 0.05$.

cells into osteoblasts and enhanced differentiation into adipocytes.

Because *Oc*-Cre-mediated deletion of *Pkd1* in osteoblasts would carry forward to the terminal differentiated osteocytes, we cannot exclude a possible role of the osteocyte in the bone phenotype in *Pkd1*$^{Oc\text{-}cko}$ null mice. In addition to being expressed throughout the osteoblastic lineage during embryogenesis and in postnatal bone, *Pkd1* is also expressed in chondrocytes (6). Consequently, the more severe skeletal abnormalities in global *Pkd1* null compared with *Pkd1*$^{Oc\text{-}cKO}$ mice could be due to PC1 regulation of osteoblast differentiation or chondrocyte function during development or to systemic effects caused by the presence of polycystic kidneys (6, 7). Additional studies that ablate *Pkd1* earlier in the osteoblast lineage during embryogenesis or later in osteocytes, as well in mature and immature chondrocytes, will be needed to establish a direct role of PC1 in skeletal development and to establish the respective contributions of PKD1 function in preosteoblasts, osteoblasts, osteocytes, and chondrocytes.

We previously demonstrated that PC1 selectively regulates *Runx2*-II P1 promoter activity in osteoblasts through an intracellular calcium pathway linked to nuclear factor I family and AP-1 transcription factors (17). The PC1 regulates a variety of signal transduction pathways in renal epithelial cells, including Akt1 and GSK3β (26–28), which are also important regulators of bone mass (42, 43). The present studies indicate that *Pkd1* also regulates PI3K-Akt-GSK3β signaling in osteoblasts and that this pathway is upstream of Runx2. The decline in Akt-GSK3β-β-catenin signaling in osteoblasts from *Pkd1*$^{Oc\text{-}cko}$ null mice and the finding that PC1-PI3K-Akt signaling regulates *Runx2*-II P1 promoter activity suggest that this may represent another PKD1-dependent pathway regulating osteoblast function. The interactions between WNT- and PKD1-dependent signaling pathways, however, are complex, and further studies will be needed to define the mechanism whereby loss of polycystin 1 results in decreased β-catenin activity.

The broader role of PC1 in regulating bone physiology is not revealed by our studies. There is no known ligand for PC. Polycystin potentially functions as a mechanosensor, a chemosensor, or as a sensor of cell-cell or cell-matrix interactions (44, 45). PC1 colocalizes to the primary cilium (46), which is also present in osteoblasts, osteocytes, and chondrocytes (47, 48). Also, cleavage of PC1 at the G protein-coupled receptor proteolytic site upstream of the first TM segment may be required for bioactivity (49), suggesting that PC1 may be constitutively active. Although the precise activator in bone remains to be defined, PC1 presence or its ability to sense environmental cues during bone remodeling may allow it to function as a "hub" or a common connection point that permits cells in the osteoblast lineage to sense diverse environmental signals during skeletal development and translate

these into multiple signaling pathways required for maintenance of bone mass.

In contrast to the role of PKD1 in mouse bone, a PC1-dependent bone phenotype has not been reported in humans with ADPKD, who have superimposed renal osteodystrophy. It may yet be possible to detect small, clinically unapparent reductions of bone density in humans heterozygous for *PKD1* mutations prior to developing kidney failure. In addition, there are some very interesting but rare families with early onset of polycystic kidney disease in newborns that are associated with severe skeletal malformations, similar to those observed in mice with homozygous *Pkd1* mutations, suggesting that broadly disrupting both alleles in osteoblasts/osteocytes (analogous to the *Pkd1* null mouse as opposed to random second hits in ADPKD) might cause clinically apparent bone disease in humans (12, 50).

In conclusion, the finding that selective reduction of *Pkd1* in osteoblasts results in osteopenia defines a new signaling paradigm in bone that has the potential to expand our understanding of how bone senses environmental signals maintaining bone mass as well as regulating osteoblast growth and development. The further study of polycystin function in bone could provide a variety of new insights, ranging from new mechanosensing mechanisms potentially involving primary cilium to identifying a molecular target for the development of pharmacological approaches to increased bone mass in osteopenic disorders.

Acknowledgments—We are particularly grateful to Dr. Gregory Germino at Johns Hopkins University for providing the floxed Pkd1 mice.

REFERENCES

1. Xu, H., Shen, J., Walker, C. L., and Kleymenova, E. (2001) *DNA Seq.* **12,** 361–366
2. Chauvet, V., Qian, F., Boute, N., Cai, Y., Phakdeekitacharoen, B., Onuchic, L. F., Attié-Bitach, T., Guicharnaud, L., Devuyst, O., Germino, G. G., and Gubler, M. C. (2002) *Am. J. Pathol.* **160,** 973–983
3. Wilson, P. D. (2004) *N. Engl. J. Med.* **350,** 151–164
4. Gabow, P. A. (1993) *N. Engl. J. Med.* **329,** 332–342
5. Torra, R., Badenas, C., San Millán, J. L., Pérez-Oller, L., Estivill, X., and Darnell, A. (1999) *Am. J. Hum. Genet.* **65,** 345–352
6. Lu, W., Shen, X., Pavlova, A., Lakkis, M., Ward, C. J., Pritchard, L., Harris, P. C., Genest, D. R., Perez-Atayde, A. R., and Zhou, J. (2001) *Hum. Mol. Genet.* **10,** 2385–2396
7. Boulter, C., Mulroy, S., Webb, S., Fleming, S., Brindle, K., and Sandford, R. (2001) *Proc. Natl. Acad. Sci. U.S.A.* **98,** 12174–12179
8. Peczkowska, M., Januszewicz, A., Grzeszczak, W., Moczulski, D., Janaszek-Sitkowska, H., Kabat, M., Biederman, A., Hendzel, P., Prejbisz, A., Cendrowska-Demkow, I., Zieliński, T., and Januszewicz, M. (2004) *Blood Press* **13,** 283–286
9. van Dijk, M. A., Chang, P. C., Peters, D. J., and Breuning, M. H. (1995) *J. Am. Soc. Nephrol.* **6,** 1670–1673
10. Hassane, S., Claij, N., Lantinga-van Leeuwen, I. S., Van Munsteren, J. C., Van Lent, N., Hanemaaijer, R., Breuning, M. H., Peters, D. J., and DeRuiter, M. C. (2007) *Arterioscler. Thromb. Vasc. Biol.* **27,** 2177–2183
11. Housset, C. (2005) *Gastroenterol. Clin. Biol.* **29,** 861–869
12. Watnick, T. J., Torres, V. E., Gandolph, M. A., Qian, F., Onuchic, L. F., Klinger, K. W., Landes, G., and Germino, G. G. (1998) *Mol. Cell* **2,** 247–251
13. Driscoll, J. A., Bhalla, S., Liapis, H., Ibricevic, A., and Brody, S. L. (2008) *Chest* **133,** 1181–1188
14. Kolpakova-Hart, E., McBratney-Owen, B., Hou, B., Fukai, N., Nicolae, C., Zhou, J., and Olsen, B. R. (2008) *Dev. Biol.* **321,** 407–419
15. Kolpakova-Hart, E., Nicolae, C., Zhou, J., and Olsen, B. R. (2008) *Matrix Biol.* **27,** 505–512
16. Hou, B., Kolpakova-Hart, E., Fukai, N., Wu, K., and Olsen, B. R. (2009) *Bone* **44,** 1121–1133
17. Xiao, Z., Zhang, S., Magenheimer, B. S., Luo, J., and Quarles, L. D. (2008) *J. Biol. Chem.* **283,** 12624–12634
18. Xiao, Z., Zhang, S., Mahlios, J., Zhou, G., Magenheimer, B. S., Guo, D., Dallas, S. L., Maser, R., Calvet, J. P., Bonewald, L., and Quarles, L. D. (2006) *J. Biol. Chem.* **281,** 30884–30895
19. Piontek, K. B., Huso, D. L., Grinberg, A., Liu, L., Bedja, D., Zhao, H., Gabrielson, K., Qian, F., Mei, C., Westphal, H., and Germino, G. G. (2004) *J. Am. Soc. Nephrol.* **15,** 3035–3043
20. Zhang, M., Xuan, S., Bouxsein, M. L., von Stechow, D., Akeno, N., Faugere, M. C., Malluche, H., Zhao, G., Rosen, C. J., Efstratiadis, A., and Clemens, T. L. (2002) *J. Biol. Chem.* **277,** 44005–44012
21. Xiao, Z., Awad, H. A., Liu, S., Mahlios, J., Zhang, S., Guilak, F., Mayo, M. S., and Quarles, L. D. (2005) *Dev. Biol.* **283,** 345–356
22. Glass, D. A., 2nd, Bialek, P., Ahn, J. D., Starbuck, M., Patel, M. S., Clevers, H., Taketo, M. M., Long, F., McMahon, A. P., Lang, R. A., and Karsenty, G. (2005) *Dev. Cell* **8,** 751–764
23. David, V., Martin, A., Lafage-Proust, M. H., Malaval, L., Peyroche, S., Jones, D. B., Vico, L., and Guignandon, A. (2007) *Endocrinology* **148,** 2553–2562
24. Xiao, Z. S., Hjelmeland, A. B., and Quarles, L. D. (2004) *J. Biol. Chem.* **279,** 20307–20313
25. Lantinga-van Leeuwen, I. S., Leonhard, W. N., van de Wal, A., Breuning, M. H., Verbeek, S., de Heer, E., and Peters, D. J. (2006) *Genesis* **44,** 225–232
26. Boca, M., D'Amato, L., Distefano, G., Polishchuk, R. S., Germino, G. G., and Boletta, A. (2007) *Mol. Biol. Cell* **18,** 4050–4061
27. Boca, M., Distefano, G., Qian, F., Bhunia, A. K., Germino, G. G., and Boletta, A. (2006) *J. Am. Soc. Nephrol.* **17,** 637–647
28. Kim, E., Arnould, T., Sellin, L. K., Benzing, T., Fan, M. J., Grüning, W., Sokol, S. Y., Drummond, I., and Walz, G. (1999) *J. Biol. Chem.* **274,** 4947–4953
29. Raucci, A., Bellosta, P., Grassi, R., Basilico, C., and Mansukhani, A. (2008) *J. Cell. Physiol.* **215,** 442–451
30. Westendorf, J. J., Kahler, R. A., and Schroeder, T. M. (2004) *Gene* **341,** 19–39
31. Mukherjee, A., and Rotwein, P. (2009) *J. Cell Sci.* **122,** 716–726
32. Aoki, K., and Taketo, M. M. (2008) *Methods Mol. Biol.* **468,** 307–331
33. Constantinou, T., Baumann, F., Lacher, M. D., Saurer, S., Friis, R., and Dharmarajan, A. (2008) *J. Mol. Signal* **3,** 10
34. Iwaniec, U. T., Wronski, T. J., Liu, J., Rivera, M. F., Arzaga, R. R., Hansen, G., and Brommage, R. (2007) *J. Bone Miner. Res.* **22,** 394–402
35. Kim, D., Cho, S. W., Her, S. J., Yang, J. Y., Kim, S. W., Kim, S. Y., and Shin, C. S. (2006) *Stem Cells* **24,** 1798–1805
36. Lian, J. B., and Stein, G. S. (1995) *Iowa Orthop. J.* **15,** 118–140
37. Yamaguchi, T., Wallace, D. P., Magenheimer, B. S., Hempson, S. J., Grantham, J. J., and Calvet, J. P. (2004) *J. Biol. Chem.* **279,** 40419–40430
38. Piontek, K., Menezes, L. F., Garcia-Gonzalez, M. A., Huso, D. L., and Germino, G. G. (2007) *Nat. Med.* **13,** 1490–1495
39. Nuttall, M. E., and Gimble, J. M. (2000) *Bone* **27,** 177–184
40. Rocha, V. Z., Folco, E. J., Sukhova, G., Shimizu, K., Gotsman, I., Vernon, A. H., and Libby, P. (2008) *Circ. Res.* **103,** 467–476
41. Klein, R. F., Allard, J., Avnur, Z., Nikolcheva, T., Rotstein, D., Carlos, A. S., Shea, M., Waters, R. V., Belknap, J. K., Peltz, G., and Orwoll, E. S. (2004) *Science* **303,** 229–232
42. Kawamura, N., Kugimiya, F., Oshima, Y., Ohba, S., Ikeda, T., Saito, T., Shinoda, Y., Kawasaki, Y., Ogata, N., Hoshi, K., Akiyama, T., Chen, W. S., Hay, N., Tobe, K., Kadowaki, T., Azuma, Y., Tanaka, S., Nakamura, K., Chung, U. I., and Kawaguchi, H. (2007) *PLoS One* **2,** e1058
43. Kugimiya, F., Kawaguchi, H., Ohba, S., Kawamura, N., Hirata, M., Chikuda, H., Azuma, Y., Woodgett, J. R., Nakamura, K., and Chung, U. I. (2007) *PLoS One* **2,** e837
44. Weimbs, T. (2007) *Am. J. Physiol. Renal Physiol.* **293,** F1423–F1432
45. Wilson, P. D., Geng, L., Li, X., and Burrow, C. R. (1999) *Lab. Invest.* **79,** 1311–1323

46. Li, Q., Montalbetti, N., Wu, Y., Ramos, A., Raychowdhury, M. K., Chen, X. Z., and Cantiello, H. F. (2006) *J. Biol. Chem.* **281,** 37566–37575
47. Jensen, C. G., Poole, C. A., McGlashan, S. R., Marko, M., Issa, Z. I., Vujcich, K. V., and Bowser, S. S. (2004) *Cell Biol. Int.* **28,** 101–110
48. Takaoki, M., Murakami, N., and Gyotoku, J. (2004) *Biol. Sci. Space* **18,** 181–182
49. Qian, F., Boletta, A., Bhunia, A. K., Xu, H., Liu, L., Ahrabi, A. K., Watnick, T. J., Zhou, F., and Germino, G. G. (2002) *Proc. Natl. Acad. Sci. U.S.A.* **99,** 16981–16986
50. Turco, A. E., Padovani, E. M., Chiaffoni, G. P., Peissel, B., Rossetti, S., Marcolongo, A., Gammaro, L., Maschio, G., and Pignatti, P. F. (1993) *J. Med. Genet.* **30,** 419–422